Evidence for the Role of Propagating Stress Waves during Fracture

L. C. Krysac and J. D. Maynard
Department of Physics, The Pennsylvania State University, University Park, Pennsylvania 16802
(Received 12 May 1998)

During the fracture of a brittle material, the breaking of a bond launches a propagating stress wave which may trigger the breaking of other bonds. Such a process might be important just prior to an avalanche of bond-breaking events when there would be a relatively high density of bonds on the verge of breaking. This paper reports experiments with a model brittle material where the time and location of individual bond-breaking events are measured during fracture. Evidence for the role of propagating stress waves has been found. [S0031-9007(98)07628-5]

PACS numbers: 62.20.Mk, 43.35.+d, 46.30.Nz, 81.40.Np

The problem of fracture is an old one [1], posing challenging and interesting difficulties such as an extreme sensitivity of some macroscopic properties to the presence of microscopic defects and disorder. For example, disordered materials composed of bonds with a random distribution of strengths, such as concrete, ceramics, and polycrystallines, exhibit a broad range of fracture strength [2]. Recent advances in the statistical physics of disordered systems applied to the problem of fracture have generated theoretical and experimental interest among physicists [2,3]. In testing and extending many current theories, it would be clearly advantageous to be able to observe and record individual bond-breaking events, locating them in time and space. We present here experimental observations of bond-by-bond breaking and evidence for the role of propagating stress waves during the fracture of an open cell carbon foam. This material may be considered as a large-scale version of systems which consist of an array of elements with a random bond strength distribution. Although the carbon foam may not be an appropriate analog of some materials, it is interesting in its own right as a brittle material and it does provide a model system for testing theories.

The glassy carbon foam is a commercial product produced from burning polyurethane foam in an inert gas, leaving behind a network of brittle struts which loosely form unit cells in the approximate shape of pentagonal dodecahedrons [4,5]. An illustration of a thin slice of the foam is shown in the inset of Fig. 1. The struts, of varying tensile strengths, play the role of the bonds. The nominal distribution of bond strengths, measured by vertical loading of individual struts on the bottom of a hanging bulk sample, is shown by the histogram in Fig. 2. The number of bonds represented is normalized to the average count of the total number of bonds broken over the fracture surface of a sample. By fitting a Weibull distribution [2,6] to the cumulative sum of the measured bond strength distribution, a fit to the histogram was obtained. The solid line in Fig. 2 shows dn/dS, the number of bonds per unit area which will break when a stress between S and $S + dS$ is applied to it, versus S.

Cylindrical samples of the foam with a diameter of 5.04 cm were fractured under tensile force while suspended in a 1 m^3 tub of water; the system is illustrated in Fig. 1. The samples were suspended from large springs at the center of the tub, far from the sound-reflecting walls and water surface. The water allowed acoustic signals originating from breaking struts within the interior of the sample to propagate, with only slight damping (e.g., relative to air) through the millimeter-sized pores. The springs ensured that for small changes in strain, the applied stress would stay approximately constant. The applied stress F (applied force divided by the cross-sectional area of the

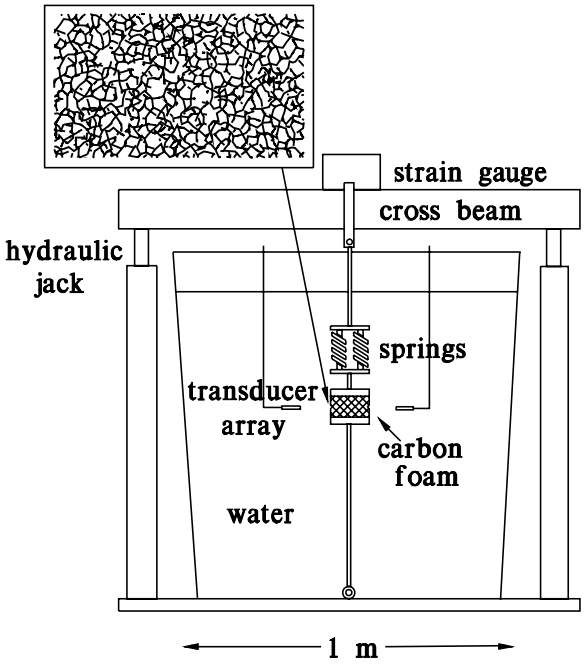

FIG. 1. A schematic depiction of the apparatus, consisting of a 1 m^3 tub for water, two hydraulic jacks and a cross beam which apply the tensile stress, a strain gage which measures the applied stress, the cylindrical carbon foam sample which is suspended and immersed in water far from sound reflecting walls and surfaces, and an array of transducers which collect the acoustic signals generated by breaking carbon bonds. The inset illustrates a thin slice of the foam.

 0031-9007/98/81(20)/4428(4)$15.00

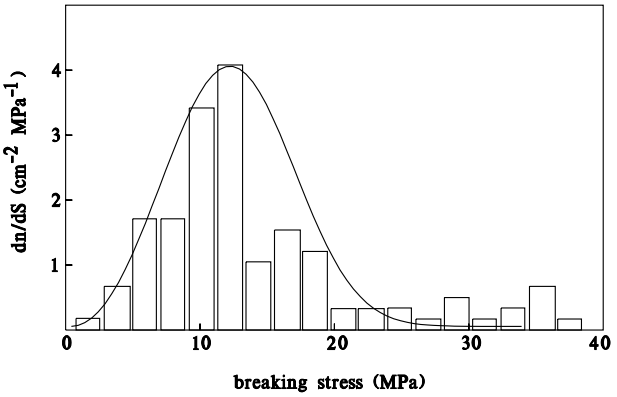

FIG. 2. The measured distribution of bond strengths (histogram) for the open cell carbon foam material, measured by vertical loading of individual struts. Also shown (solid line) is dn/dS (cm^{-2} MPa^{-1}), the density of bonds per unit area per unit stress, which fits the measured histogram.

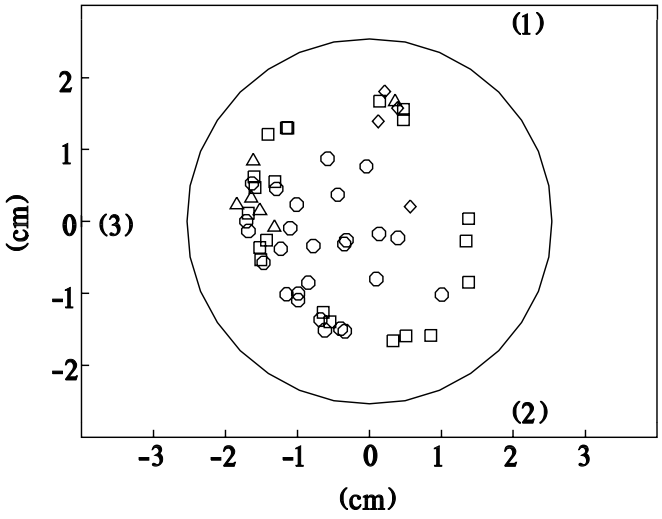

FIG. 3. The location of bond-breaking events, deduced from acoustic triangulation, near the fracture plane of one sample. Early stages of fracture are represented by diamonds, squares, and triangles, as discussed in the text. The events recorded just prior to the sample rupturing are indicated with circles. The transducers recording the acoustic bursts are indicated with the labels (1), (2), and (3).

sample) was measured with a calibrated strain gage and was increased, using hydraulic jacks, by small incremental steps until, at a final applied stress F_f, there was a large avalanche of bond-breaking events and the sample ruptured in half. After each small change in stress, the stress was kept constant until precursor bond-breaking events had ceased. A 0.79 cm notch was scored into the cylindrical samples, forming a waist at the sample midsection, so that the samples would preferentially cleave in the plane of the notch; it was found that out-of-plane deviations were limited to ± 5 bond lengths (a few mm). Surrounding the sample in the plane of the waist was an array of wideband 35 MHz piezoelectric acoustic transducers (1 mm diameter) [7]. The transducers were arranged symmetrically at a distance of 1 cm from the sample and collected the acoustic signals, typically consisting of 50 ± 20 μs bursts of $\sim$1 MHz sound, generated by isolated single bond-breaking events within the carbon foam. These signals could be well characterized by deliberately breaking single struts and observing the resulting acoustic burst after it had propagated through some thickness of foam, and comparing with similar signals observed during the fracture process. Single bond-breaking events could be recorded and counted up to a relatively short instant before the final rupturing event. From the recorded signals, the relative timing and location of successive bond-breaking events could be found with a straightforward geometric triangulation procedure using the arrival times of the acoustic signals at three different transducers in the array. Figure 3 shows the triangulated position of a number of such single bond-breaking events on one sample. Events occurring early in the fracture process are indicated in Fig. 3 with diamonds, squares, and triangles (corresponding to F/F_f of 0.70, 0.90, and 0.97); as will be discussed later, these occur as individual events, widely spaced in time. Events occurring later, as the externally applied load increases towards the rupturing stress, are indicated with circles in Fig. 3 (corresponding to F/F_f of 0.99); also discussed later, these tend to be closely spaced in time. The final rupturing catastrophe, where typically about 90% of the bonds were broken, produced a larger amplitude burst lasting several milliseconds. The results presented in this paper are based on the observation and spatial-temporal location of over 220 single bond-breaking events which occurred before the final rupturing event of five samples. It should be noted that the value of the applied stress at the final rupture F_f was different for each sample.

The ratios of the relative separation in space and the separation in time, or the "speed," between successive precursors are shown in Fig. 4 with the sequence of letters (a) to (d) indicating the approach of the applied stress F to F_f. Early in the fracture process, with F far from F_f, the timing between precursors is large, peaking at about 300 ms, which is set by the rate of the manual changes in stress. When combined with the distance between the sites of successive precursors, this produces a peak at an effective "speed" of about 0.03 m/s in Figs. 4(a), 4(b), and 4(c). Figure 4(d) shows that as the fracture process continues, with the applied stress approaching F_f, the timing between successive precursors becomes small, shifting the peak in effective speed by 4 orders of magnitude to about 10^3 m/s, which is on the order of the average speed of sound in the carbon foam material itself. A separate measurement of the average speed of sound in the foam was done by deliberately breaking single bonds in a bulk sample and recording, with an acoustic transducer pressed against a strut some distance away, the arrival of the resulting impulsive stress wave. This measurement is shown in Fig. 4(e) for comparison with Figs. 4(a), 4(b),

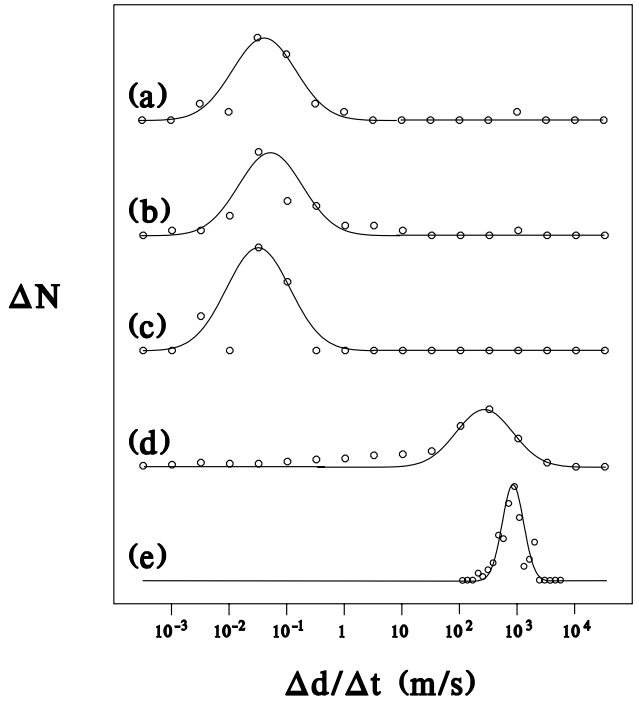

FIG. 4. The ratio of the spatial separation and time delay between successive bond-breaking events for increasing externally applied tensile stress [(a)–(d)]. Also shown is the measured speed of sound within the carbon material (e). At low stress [(a)–(c)] successive bond-breaking events occur at low speed, while at high stress (d) they become correlated with the speed of sound (e). The number of events used to generate the curves (a) through (e) were 19, 34, 6, 165, and 200, respectively.

$4(c)$, and $4(d)$. Since the material is disordered, the stress wave originating at the break site must travel a tortuous route through the material. This produces a spread in the measured sound speed, with the average speed ($\sim$1000 m/s) somewhat less than the maximum speed ($\sim$2000 m/s) set by the true speed of sound through the carbon material. There is a clear overlap between the peak in Fig. $4(d)$ with the stress wave average speed shown in Fig. $4(e)$. This overlap suggests that as the fracture process reaches a high density of bonds about to break (e.g., prior to an avalanche), stress waves generated by the breaking of bonds play a role in the subsequent breaking of bonds. This is a key form of evidence for the role of propagating stress waves during fracture, involving their speed. The question arises as to why the typical time between bond breaking events changes when the applied tensile stress approaches its maximum value. The answer leads to supporting evidence for the role of propagating stress waves during fracture, which involves their amplitude and attenuation, as discussed next.

The stress released when a strut breaks was observed to consist primarily of a leading impulsive oscillation, whose positive excursions exceeded the eventual static stress in the new equilibrium state. From the observed maximum amplitude of acoustic signals generated by breaking struts in the surrounding water, about 0.003 MPa, the amplitude of the stress waves in the carbon material itself may be estimated. Approximating the carbon struts as cylinders with radius $a \sim 0.03$ cm [5], the break site along the strut will radiate primarily as a dipole source, for which the ratio of the acoustic power emitted into the water P_w to the acoustic power emitted within the carbon P_c is estimated [8] with

$$P_w/P_c \sim (a/\lambda)^4, \tag{1}$$

where $\lambda \sim 0.19$ cm is the typical wavelength of the emission. Thus, the measured amplitude of sound into the water gives the maximum amplitude of the impulsive portion of the stress waves in the carbon S' as about 0.12 MPa. This impulsive change in stress travels at the sound speed in the foam and acts only on nearby bonds where its amplitude is large. The outwardly spreading stress pulse undergoes significant acoustic attenuation since it must propagate through the highly disordered, tortuous network of struts, enhancing the effects of ordinary acoustic damping mechanisms. The acoustic attenuation occurs over a characteristic length scale l_a, which was determined experimentally (by breaking a bond manually and measuring signals in the carbon with transducers located at varying distances) to be 0.85 ± 0.2 cm. Assuming that the propagating stress wave can trigger other bonds in the fracture plane only over an area given by πl_a^2, and that the density of bonds which may be triggered by a stress wave of amplitude S' is $(dn/dS)S'$, then the number of bonds which may be triggered by the attenuated stress wave is

$$N' = \pi l_a^2 (dn/dS) S'. \tag{2}$$

The triggered bonds will be the source of stress waves which may in turn trigger other events, as in an avalanche of bond-breaking events. The threshold for such triggering is set by the requirement that $N' \geq 1$, which gives a minimum value $(dn/dS)_{\min}$ of the density of bonds per unit area per unit stress:

$$dn/dS \geq 1/\pi l_a^2 S' \equiv (dn/dS)_{\min}. \tag{3}$$

From the measured acoustic attenuation length l_a and the estimated amplitude of the impulsive stress pulse S', the threshold value of $(dn/dS)_{\min}$ is determined as 3.6 ± 1.5 cm^{-2} MPa^{-1}.

At this point we must consider the fact that the stress is not uniform over the sample midsection; because of the notch cut around the sample, the stress is higher on the outermost bonds of the midsection (i.e., at the tip of the notch). We have calculated the static stress distribution for our samples using a finite element analysis [9] (appropriate for our network of discrete bonds), and have found that the very outermost bonds get a stress which is seven times that of the bulk of the bonds in the midsection, the next outermost bonds get a stress which is twice that of the bulk, and the rest do not differ appreciably from the bulk. As the external stress is increased

TABLE I. The final rupturing stress F_f and the cumulative number of bond-breaking events N for five carbon foam samples.

Sample no.	Rupture stress (MPa)	Number of bonds
1	0.819	63
2	0.459	65
3	0.604	57
4	0.898	54
5	0.649	32

from zero, the high stress value at the tip of the notch moves through the peak in the bond-strength distribution curve (Fig. 2), and bonds preferentially break at the tip of the notch. This is demonstrated in our experimental data by the diamonds, squares, and triangles in Fig. 3. As the external stress reaches a value just below that of the final rupture, the situation is quite different. Now the high stress value at the tip of the notch is well into the tail of the distribution (around 35 MPa in Fig. 2), and the stress value for the bulk of the bonds (with stress around 5 MPa) has moved toward the peak of the distribution in Fig. 2. Now bonds which are on the verge of breaking may be found anywhere in the sample midsection; this is demonstrated in our experiment by the more uniform distribution of the circles in Fig. 3. Because the bulk of the bonds with uniform stress occupy 90% of the sample midsection just prior to the final rupture, considering just these bonds in our analysis will incur an error no greater than that of our estimate of $(dn/dS)_{\min}$ determined in the preceding paragraph.

If a minimum threshold value exists for (dn/dS), then there must also exist a cumulative number N of bond-breaking events which may occur before stress waves may trigger other bonds which are on the verge of breaking. The cumulative number is given by

$$N = \int \int_0^{S_f} \frac{dn}{dS}\, dS dA\,, \tag{4}$$

where S_f corresponds to $(dn/dS)_{\min}$ for the bulk of the bonds, and the integral with respect to area dA is over the sample midsection. Thus, our samples will be able to withstand a characteristic number of precursor broken bonds before stress waves begin to play a role (just before the final rupture for our samples). Table I shows the stress at the final rupture as well as the cumulative number of precursor single bond-breaking events N occurring before the final rupture for five similar carbon foam samples which were fractured under similar conditions. For the fifth sample listed, the number of detected bond-breaking events is an undercount due to an initial misalignment of the transducer array during the early stages of fracture. The average tensile stress required to rupture the foam samples was 0.70 ± 0.20 MPa, with or without the fifth sample included, varying by 25%. By contrast, the average number of precursor broken bonds detected, excluding the anomalous low count, was 60 ± 5, varying by only 8%. The number of bonds broken before the final rupturing event may be measured more easily than the final stress on the bulk of the bonds. Using Eq. (4), this cumulative number of bonds corresponds to a value for the minimum density of bonds per unit area per unit stress $(dn/dS)_{\min}$ of $2.35 \pm 0.1\ \mathrm{cm}^{-2}\,\mathrm{MPa}^{-1}$, which is within error of our estimate above. It should also be noted that the stress corresponding to this value in Fig. 2 is close to the stress predicted by the finite element analysis for the bulk of the bonds near the final rupture. These results give significant support to the evidence for the role of propagating stress waves in fracture.

Thanks to Ultramet, Pacoima, CA 91331 for supplying the carbon foam. Also thanks to Jayanth Banavar for helpful suggestions, and to undergraduate participants Kirk Fischer, Mike Marrotta, Christina D'Arrigo, Ivonne D'Amato, Ben Winjum, Jen Linton, and Jill Kuzo. This research was supported by The Office of Naval Research and NSF DMR 9306791.

[1] G. Galilei, *Two New Sciences, Including Centers of Gravity and Force of Percussion*, orig. 1638, translated by S. Drake (University of Wisconsin P., Madison, WI, 1974).

[2] *Statistical Models for the Fracture of Disordered Media*, edited by H. J. Herrmann and S. Roux (North-Holland, Amsterdam, 1990), and references therein.

[3] L. de Arcangelis and S. Redner, J. Phys. Lett. **46**, L-585 (1985); J. Fineberg, S. P. Gross, M. Marder, and H. L. Swinney, Phys. Rev. Lett. **67**, 447 (1991); Phys. Rev. B **45**, 5146 (1992); S. P. Gross, J. Fineberg, M. Marder, W. D. McCormick, and H. L. Swinney, Phys. Rev. Lett. **71**, 3162 (1993); A. Buchel and J. P. Sethna, Phys. Rev. Lett. **77**, 1520 (1996); D. Holland and M. Marder, Phys. Rev. Lett. **80**, 746 (1998); M. Marder and J. Fineberg, Phys. Today **49**, No. 9, 24 (1996); S. Ramanathan, D. Ertas, and D. S. Fisher, Phys. Rev. Lett. **79**, 873 (1997); J. V. Andersen, D. Sornette, and K. Leung, Phys. Rev. Lett. **78**, 2140 (1997); W. A. Curtin, Phys. Rev. Lett. **80**, 1445 (1998); C. Maes, A. Van Moffaert, H. Frederix, and H. Strauven, Phys. Rev. B **57**, 4987 (1998).

[4] C. R. Schmitt, Mater. Res. Standards **10**, 26 (1970).

[5] R. Brezny and D. J. Green, Acta Metall. Mater. **38**, 2517 (1990).

[6] W. Weibull, Igenors Vatenkaps Akadiens Handlingar, Proc. No. 151 (The Royal Swedish Institute of Engineering Research, Stockholm, 1939).

[7] Model VP-1093 Pinducer, Valpey-Fisher Corp., 75 South Street, Mopkinton, MA 01748.

[8] P. M. Morse and H. Feshbach, *Methods of Theoretical Physics, Part II* (McGraw-Hill, New York, 1953), p. 1479.

[9] O. C. Zienkiewicz, *The Finite Element Method* (McGraw-Hill, London, 1997); T. R. Chandrupatla and A. D. Belegundu, *Introduction to Finite Elements in Engineering* (Prentice Hall, Englewood Cliffs, NJ, 1997).